Case Studies in Construction Materials 24 (2026) e06166

Contents lists available at ScienceDirect

Case Studies in Construction Materials

journal homepage: www.elsevier.com/locate/cscm

Experimental study on the mechanical and microstructural properties of lightweight hybrid fibre reinforced concrete

Salman Alnasser [a,*], Suhaila Mattar [a], Aref A. Abadel [b]

[a] School of Civil Engineering, Faculty of Engineering, University of Leeds, Leeds, UK
[b] Department of Civil Engineering, College of Engineering, King Saud University, Saudi Arabia

ARTICLE INFO

Keywords:
Lytag
Leca
Lightweight aggregate
Lightweight aggregate concrete
Hybrid fibre reinforcement
Mechanical properties
Fracture toughness

ABSTRACT

The utilisation of lightweight materials to reduce building weight results in cost savings, enhanced efficiency, and energy conservation. It also mitigates damage from natural hazards such as earthquakes and reduces problems associated with structural overload. This research aims to develop sustainable lightweight aggregate concrete (LWAC) incorporating hybrid fibres and two lightweight aggregates (Lytag and Leca). Two fibres type were used: basalt fibres (BF) with lengths of 48 mm and two types of polypropylene fibres with lengths of 20 mm (PPX fibre) and 40 mm (PPD fibre). The performance of LWAC was experimentally evaluated in terms of modulus of elasticity, compressive strength, splitting tensile strength, flexural strength, fracture toughness, and microstructural characteristics. Ten distinct mixtures were designed, and 150 LWAC samples (cubes, cylinders, and prisms) were tested. The results showed that all oven-dried densities are below 1930 kg/m^3, meeting the definition of LWAC as outlined by the BS EN 206. Specimens made with Lytag aggregate significantly outperformed those with Leca aggregate, exhibiting enhancements in modulus of elasticity, compressive strength, splitting tensile strength, and flexural strength of 31.1%, 61%, 47.2%, and 23.6%, respectively. Fibres inclusion had little effect on compressive strength, but significantly enhanced splitting tensile strength (up to 37.9%), flexural strength (up to 34.3%), and energy absorption capacity (up to 71.8%). Mixtures containing 0.5% BF + 1.0% PPD (regardless of the aggregate type) demonstrated the best performance among the fibre-reinforced LWAC specimens.

1. Introduction

The growing demand for housing and infrastructure, coupled with the need for modern systems that accelerate building processes, improve efficiency, and strengthen reinforced concrete (RC) structures against earthquakes, has become a critical concern. Understanding the impact of lightweight materials on RC structures has become an important focus within the construction sector and civil projects, drawing considerable attention from both researchers and engineers incorporating lightweight materials reduces the overall weight of buildings, which in turn lowers the construction costs, enhance time and energy efficiency, and improve structural performance. In addition, it helps mitigate earthquake induced damage and minimize problems related to structural overloading. Lightweight aggregates concrete (LWAC) is increasingly used in both non-structural and structural members such as columns and beams, leading to reduction in the overall weight and dimensions of RC structures [1–4]. LWAC can be produced using lightweight

* Corresponding author.
E-mail address: cnsal@leeds.ac.uk (S. Alnasser).

https://doi.org/10.1016/j.cscm.2026.e06166
Received 4 November 2025; Received in revised form 20 December 2025; Accepted 19 May 2026
Available online 21 May 2026

aggregates (LWA) and supplementary cementitious materials [3,5]. The predominant approach involves the utilisation of LWA, which can be either natural or artificial [4,6]. Considerable research has been investigated natural aggregates such as diatomite, scoria, and pumice, as well as artificial aggregates including slag, shale, perlite, and expanded clay, for use in the concrete production [7–10].

The incorporation of LWA creates a porous framework in the LWAC, lowering density but also reducing compressive strength, while the reduction in density enables the construction of taller structures [11], it is essential to maintain a balance between the density reduction and the strength. Enhancing strength while reducing density remains a key research challenge. Fibre serves as a widely utilised strengthening approach in composites, effectively addressing the reduction in strength. In addition, concrete exhibits significant weaknesses, particularly characterised by its low tensile strength, limited strain capacity, and brittleness when subjected to compressive or flexural loads. These properties can lead to abrupt failures in RC structures during seismic events [12–15]. A viable approach to address this issue involves the utilisation of RC structures combined with various types of fibres [16,17]. The utilisation of fibre has gained significant traction in industrialised nations since the early 1960s, with advancements in the type, shape, and fabrication methods of these fibres evolving over the decades [18,19]. Basalt fibre (BF), produced by melting basalt rocks, has emerged as a sustainable alternative with minimal industrial and environmental impact. The higher silica content in the basalt components indicates that fibres derived from it are suitable options and exhibit compatibility with the cementitious matrix [20,21]. Polypropylene fibre (PPF) is a synthetic fibre characterised by excellent ductility and deformation capabilities. It can increase the concrete's ductility and durability while lowering plastic shrinkage. In comparison to steel fibres, it possesses a low cost and superior corrosion resistance [22,23]. Upon the addition of fibres into the concrete matrix, two distinct types of cracking may manifest: one occurring perpendicular and parallel to the fibres. Consequently, when the fibres intersect the crack edges perpendicularly, their bridging capability preserves the fracture's integrity, enabling significant deformations and consequently enhancing the flexural strength of the concrete due to the fibres' bridging characteristic [21,24]. The incorporation of fibres in a concrete matrix markedly enhances its resistance to cracking under various environmental circumstances [25,26]. For example, in hot and dry climates, the fibres control the main or secondary age cracks resulting from shrinking. The incorporation of a specific type of fibre improves the mechanical characteristics of concrete, albeit within a constrained spectrum. In contrast, adding hybrid fibres with multiple types exhibits the synergistic interactions of each fibre type, resulting in superior characteristic. The incorporation of hybrid fibres with varying lengths and dimensions presents a viable strategy to mitigate the issue of cracking that can arise at multiple sizes and loading stages in concrete [27–29].

Madandoust et al. [30] studied the influence of various curing circumstances on the mechanical characteristics of LWAC that incorporates expanded clay aggregate and fibres (PPF and steel (SF)). The findings indicated that the LWAC achieved optimal mechanical strength when subjected to vapor treatment at 90°C. Furthermore, the ideal proportions of SF for achieving maximum compressive and tensile strength in LWAC were determined to be 1% and 3%, respectively. Furthermore, Li et al. [31] investigated the fracture behaviour of LWAC that incorporates PPFs when subjected to high temperatures. The findings revealed that the inclusion of PPF in the LWAC at elevated temperatures resulted in a reduction of the compressive strength. Furthermore, the LWAC with PPF at ambient temperature resulted in an enhancement of the fracture energy. Conversely, a rise in fracture energy at elevated temperatures has been noticed for non-reinforced concrete incorporating PPF. Badogiannis et al. [32] study the mechanical strength of LWAC that incorporates pumice, reinforced with SF and PPF fibres. The findings indicated that the compressive strength improved by 16–76% and 47–110% for the compressive strength and flexural strength of the fibre-reinforced LWAC, respectively. They also noted that the addition of fibres had an insignificant impact on the modulus of elasticity and Poisson’s ratio. A further investigation by Libre et al. [33] examined the mechanical characteristics of LWAC with natural pumice and hybrid fibre (SF and PPF). The study demonstrated that the inclusion of fibres decreased the likelihood of segregation among the aggregates in the LWAC mixture. Additionally, the inclusion of less than 0.2% PPFs did not influence the mechanical characteristics; however, an increase to 0.5% resulted in enhanced flexural strength and toughness. Xu et al. [11] reported that BF reinforcement enhanced the compressive strength of LWAC by 62.43% compared with LWAC without fibre (control sample). In addition, the compressive strength of LWAC with BF was found to be 16.71% greater than that of the LWAC with the same length and content of PPF. BF demonstrates a greater efficacy in enhancing the mechanical characteristics of LWAC.

Zhao et al. [34] investigated the performance of lightweight ultra-high-performance concrete containing waste glass powder. They reported that the inclusion of 1.5 vol% steel fibres significantly improved mechanical performance, resulting in a 185% enhancement in compressive toughness and a remarkable 789% increase in peak strain, demonstrating pseudo-strain hardening behaviour in axial tension. In addition, while polypropylene fibres lost all mechanical qualities because of interfacial flaws, polyethylene fibres increased flexural strength by 136% through nanoscale crack bridging. Zhang et al. [35] studied the mechanical properties of lightweight cement concrete. The findings demonstrated that adding fibres successfully decreased LCC's brittleness without changing its composition. End-hooked steel fibre showed superior improvements in the mechanical properties of lightweight cement concretes compared to smooth steel and polypropylene fibres. Chen et al. [36] conducted an experimental test on the durability of ultra-high-strength lightweight geopolymeric composites. The results show that the compressive strength increased while the durability of the mixtures decreased with the addition of polypropylene and polyethylene fibres, accompanied by increased porosity. In addition, another study by Chen et al. [37] reported that under tensile or flexural loading, ultra-high-strength lightweight geopolymeric composites exhibited pseudo-strain hardening due to the presence of polyethylene fibres. Zhang et al. [38] investigated the dynamic behaviour of ultra-lightweight high-strength concrete. The findings demonstrated that ultra-lightweight high-strength concrete's compressive characteristics showed substantial strain-rate dependency and that the inclusion of fibres made the mixture more strain-rate sensitive, particularly at high strain rates. Moreover, increasing the fibre content consistently enhanced both the dynamic compressive strength and the dynamic increase factor. Nonetheless, there exists a lack of studies focusing on LWAC with hybrid fibres, particularly BF and PPF. The selected fibre length was based on preliminary trial mixes, which confirmed that this length provided adequate dispersion and an initial improvement in mechanical response, in line with the manufacturer's recommendations.

Table 1
Chemical composition of cementitious materials used in this study.

Material	SiO_2	Al_2O_3	CaO	Fe_2O_3	MgO	K_2O	Na_2O	MnO	SO_3	P_2O_5	TiO_2	LOI
CEM I	31.52	13.33	38.81	1.05	7.23	0.61	0.29	0.29	1.90	0.01	0.63	4.18
GGBS	18.90	4.92	65.49	2.79	1.15	0.59	0.28	0.07	3.29	0.08	0.35	1.55
50%CEM I + 50% GGBS	25.40	9.20	52.02	1.98	4.11	0.59	0.23	0.18	2.54	0.05	0.58	2.97

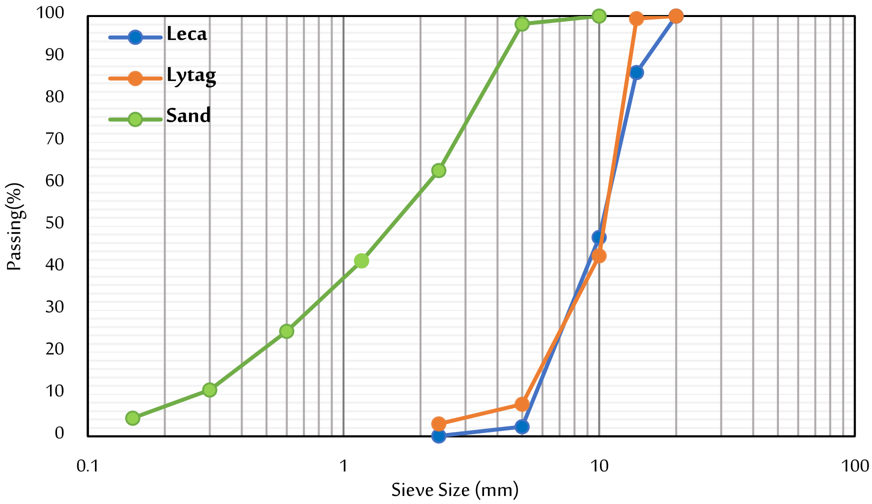

Fig. 1. The grading curves for fine and coarse aggregates used in this study.

Table 2
Physical characteristic of coarse aggregate.

Property	Aggregate size	Specific Gravity			Absorption (%)	Unit Weight (Kg/m^3)		Crushing resistance (N/mm^2)	Voids ratio (%)
		SG_{OD}	SG_{SSD}	SG_{App}		Loose	Dense		
Lytag	5/14	1.37	1.61	1.80	17.5%	892	960	11	47
Leca	5/14	1.0	1.17	1.21	19.5%	589	623	5	45

This study aims to develop LWAC using two types of LWA (Lytag and Leca) and hybrid fibres (BF, PPD and PPX). The performance of LWAC was experimentally investigated in terms of modulus of elasticity, compressive strength, splitting tensile strength, flexural strength, fracture toughness, and microstructure analysis. A total of ten mixtures and 150 samples (cubes, cylinders, and prisms) were tested to provide a comprehensive evaluation of LWAC with hybrid fibre reinforcement.

2. Materials and methods

2.1. Raw materials

2.1.1. Cementitious materials

The cement mix was consisted of 50% Ordinary Portland Cement (OPC)-CEM I (High Strength Cement 52.5 N), which is suitable for different concrete projects and complies with BS EN 197–1 standards [39]. Ground granulated blast furnace slag (GGBS) was added at a rate of 50%. The setting time test was conducted following BS EN 196–3 [40]. The initial setting time was 2 h and 28 min (148 min), while the final sitting time was 4 h and 9 min (249 min); these values meet the standards. XRF spectroscopy was used to determine the chemical composition of the cementitious materials. Table 1 provides the chemical composition of the CEM I, GGBS, and 50%CEM I + 50%GGBS.

2.1.2. Fine aggregate

The research used natural river sand as fine aggregate. Fig. 1 illustrates the grading curve for natural sand, which meets the standard limit requirements as per BS 882 (1992) [41].

Fig. 2. Lightweight aggregate used in this study: (a) Lytag; (b) Leca.

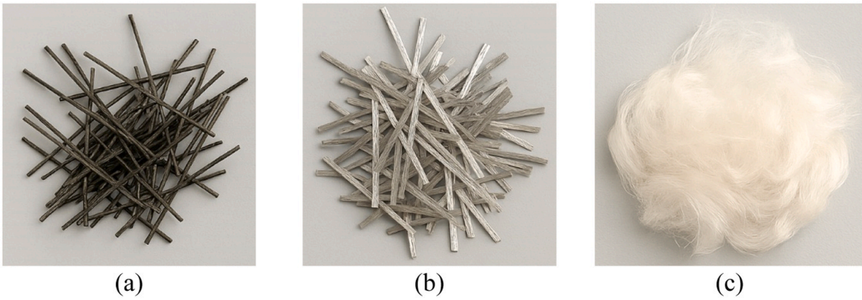

Fig. 3. Fibres used in this study: (a) BF; (b) PPD; (c) PPX.

2.1.3. Coarse aggregate

This study utilised two primary types of lightweight aggregate Lytag and Leca sourced from UK suppliers. Leca, an aggregate produced from expanded clay, and Lytag, manufactured from sintered fly ash, both contain silica (SiO_2), alumina (Al_2O_3), and iron oxide (Fe_2O_3) as their major oxides, as reported in [42]. Both aggregates contain interconnected voids that reduce density and make them suitable for lightweight concrete. Table 2 illustrates the physical characteristic of LWA. Figs. 2(a) and 2(b) show the Lytag and Leca aggregates respectively. The gradation curves for both types of aggregate are illustrated in Fig. 1; the maximum size was 14 mm for both Lytag and Leca, in accordance with BS EN 13055–1 standard [43].

2.1.4. Fibres

Two types of fibres were used in this study: basalt fibres (BF) with lengths of 48 mm and two types of polypropylene fibres with lengths of 20 mm (PPX fibre) and 40 mm (PPD fibre). The visual depiction of these fibres is illustrated in Fig. 3. The characteristics of

Table 3
Physical characteristic of fibres.

Fibre type	Shape	Length (mm)	Diameter (μm)	Elastic modulus E (GPa)	Specific gravity (kg/m^3)	Tensile strength (MPa)
BF	Round	48	13 ± 1	90–100	1900	2670
PPX	Round	20	22	≥ 3	905	380
PPD	Rectangular	40	1 × 0.5 mm (flat)	6	920	470

Table 4
Test matrix and mix proportions for LWAC mixtures kg/m^3.

Specimen ID		OPC	GGBS	Water (L/m^3)	Sand	Coarse Aggregate		Fibres		
						Lytag	Leca	BF	PPD	PPX
Group 1	LY-C0	245	245	220	620	450	-	-	-	-
	LY-B0.5D1.0	245	245	220	620	450	-	0.5%	1.0%	-
	LY-B1.0D0.5	245	245	220	620	450	-	1.0%	0.5%	-
	LY-B0.5D0.5	245	245	220	620	450	-	0.5%	0.5%	-
	LY-B1.0 × 0.5	245	245	220	620	450	-	1.0%	-	0.5%
Group 2	LE-C0	245	245	220	620	-	450	-	-	-
	LE-B0.5D1.0	245	245	220	620	-	450	0.5%	1.0%	-
	LE-B1.0D0.5	245	245	220	620	-	450	1.0%	0.5%	-
	LE-B0.5D0.5	245	245	220	620	-	450	0.5%	0.5%	-
	LE-B1.0 × 0.5	245	245	220	620	-	450	1.0%	-	0.5%

Superplasticiser: The amount ranges from 0.1% to 0.3% of the weight of OPC, depending on the mixture requirements.

Fig. 4. The specimens after casting.

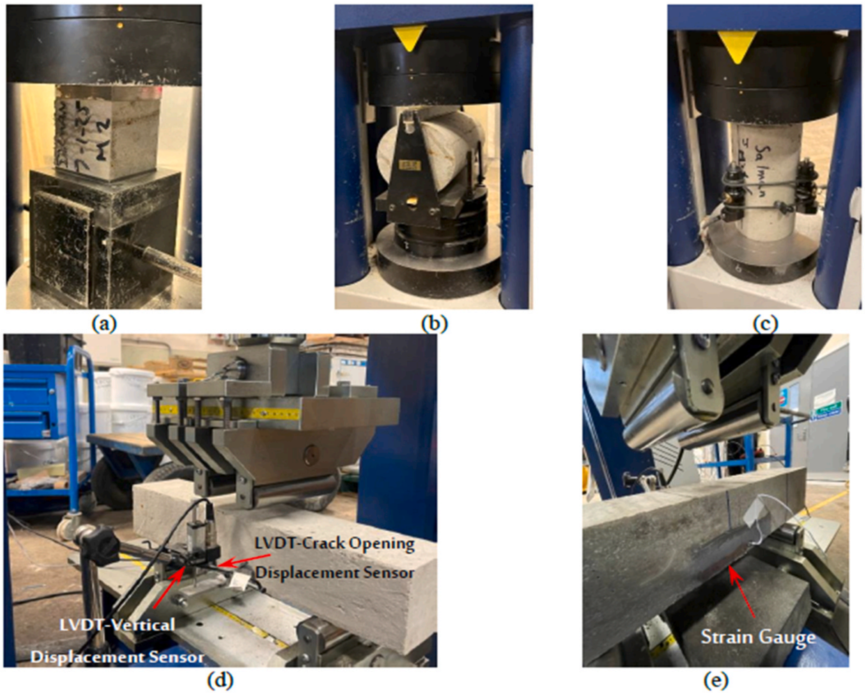

Fig. 5. Tests setup: (a) Compression Test; (b) Splitting tensile test; (c) Modulus of elasticity test; (d) Flexural strength test; (e) Strain gauge position.

basalt and polypropylene fibres, obtained from manufacturer reports, are provided in detail in Table 3. According to the manufacturers' Environmental Product Declarations (EPDs), the PP fibres used in this study have an embodied carbon of 1.95 kg CO_2-eq/kg, while the basalt fibres have an embodied carbon of 1.74 kg CO_2-eq/kg, supporting their use as relatively low-impact materials.

2.1.5. Admixture

The study used a superplasticiser known as Sika Visco Crete 25 MP, classified as a high-range water-reducing admixture that meeting the standards set by BS EN 934–2 (2009) to facilitate workability of the concrete [44].

2.2. Mix proportioning

The concrete mixtures were designed according to ACI 211.2–98 (2004) [45] and tested to find the desired workability while also meeting the specified compressive strength requirements, aiming for a target compressive strength of about 35 MPa at 28 days. The slump tests for each concrete mix were conducting in according to BS EN 12350–2 (2009) [46]. The slump of the mix was maintained within 100 mm ± 25 mm. According to BS EN 206 [47] the slump of LWAC classifies as S3. The water-to-cement ratio was 0.45 for all mixtures. The fibres were added at a volume fraction of 1.0–1.5%, which was distributed between the various fibre types. Table 4

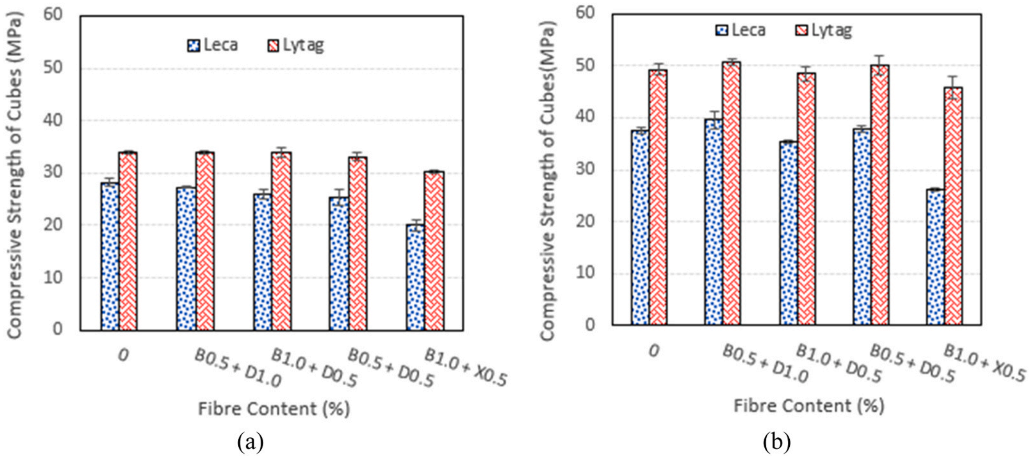

Fig. 6. Compressive strength values: (a) At 7 days; (b) At 28 days.

illustrates the components and proportions of all mixtures. In addition, the test matrix of this study is shown in Table 4. This study investigated ten concrete mixtures divided into two groups. The first five mixtures (Group 1) were prepared using Lytag aggregate, and the other five mixtures (Group 2) were prepared using Leca aggregate. The specimen ID consists of letters and numbers. The first part represents the type of lightweight aggregate, where "LY" refers to specimens with Lytag aggregate and "LE" refers to specimens with Leca aggregate. The second part represents the fibre types and their volume fraction, where "B" refers to BF, "D" refers to PPD, and "X" refers to PPX fibres. For example, LY-C0 and LE-C0 refer to control specimens in Group 1 and Group 2, respectively, LY-B1.0D0.5 refers to the specimen with a Lytag aggregate and 1.0% BF and 0.5% of PPD fibres.

2.3. Specimen preparation

All materials were carefully prepared and measured, with an extra 10–15% included to account for possible losses. A drum mixer was used to prepare the concrete samples under laboratory conditions of 20 ± 5°C and a relative humidity of at least 50%, as specified by BS 1881–125 (2013) [48]. The mixer was used to combine all dry elements, excluding cement, which was then added and mixed to ensure a homogeneous batch. The superplasticiser was dissolved in the water and gradually added to the mixture while the mixer operates. Finally, the fibres were added while mixing continued. The components were fully blended for a duration of 8–10 min before placing the concrete into the moulds. Fig. 4 shows the specimens after casting. Each specimen was stored at 20 ± 2°C and demoulded after 24 h, then placed under a relative humidity of no less than 95% for a curing period of 28 days, in accordance with BS EN12390–2 (2009) [49].

2.4. Testing method

Fig. 5 shows the test setup used in this study. The compressive strength test was conducted on cube specimens (100 × 100 × 100 mm) after 7 days and 28 days, in accordance with BS EN 12390–3 (2009) [50]. The loading rate was 0.6 ± 0.2 MPa/s. The splitting tensile test was conducted on cylinder specimens (150 × 300 mm) in accordance to BS EN 12390–6 (2009) [51]. Three cylinders per mixture were tested at 28 days. Initially, the specimen was placed in a rig designed to position it accurately at the center of the machine, and the specimen was then placed in the testing machine, as shown in Fig. 5(b). The load was applied statically at a rate of 0.06 ± 0.04 MPa/s. Concrete cylinder specimens (150 × 300 mm) were used to measure the modulus of elasticity after 28 days following BS EN 12390–13 (2009) [52]. A compression testing machine applied the load while measuring deformation, as shown in Fig. 5(c). The loading rate increased at a constant rate of (0.6 ± 0.2 MPa/s). Flexural strength was tested using prismatic beams (100 × 100 × 500 mm) under four-point load bending, in accordance with BS EN 12390–5 outlined (2009) [53]. Three prisms per mixture were tested at 28 days. The load was applied using a hydraulic jack at two points, ensuring the inner span equal to one third of the total span, as shown in Fig. 5(d). The stress rate was maintained at 0.06 ± 0.04 MPa/s. Two LVDTs were used, one to measure the vertical displacement and another to measure crack opening displacement, as shown in Fig. 5(d). A strain gauge was attached to the center of the concrete surface to record the tensile strain, as shown in Fig. 5(e). Scanning electron microscopy (SEM) and energy-dispersive X-ray analysis (EDAX) spectrum analysis were carried out to examine the chemical composition of BF and PPD fibres of polished samples. In addition, the image analysis using Fiji software was conducted to assess the area fractions of aggregates, matrix, fibres, and voids of the LWAC samples. The analysed region was taken from the mid-depth of the specimen, as shown in Section 4.3.

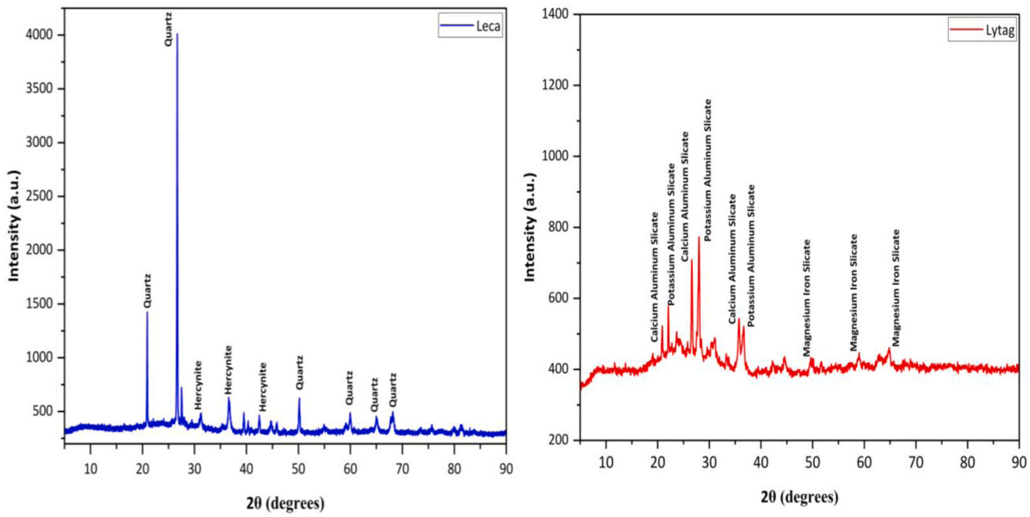

Fig. 7. XRD patterns of Leca and Lytag aggregates.

3. Results and discussion

3.1. Compressive strength

Fig. 6 illustrates the compressive strength of LWAC mixtures as ascertained from cube samples after 7 and 28 days. The compressive strengths of LY-C0 and LE-C0 specimens without fibres were 34.1 MPa and 28.3 MPa, respectively. The results showed a clear superiority of the LWAC specimens with Lytag aggregate compared to Leca aggregate, with an increase of 20.5%, as shown in Fig. 6(a). Generally, the presence of fibres has a slight effect on compressive strength. For the 7 days curing period, the Group 1 specimens (with Lytag) showed a reduction of 0.5%, 0.7%, 2.8%, and 11.2% for LY-B0.5D1.0, LY-B1.0D0.5, LY-B0.5D0.5, and LY-B1.0X0.5, respectively, compared to LY-C0 specimens. Group 2 specimens (with Leca) showed reductions of 3.5%, 8.2%, 10.5%, and 29.3% for LE-B0.5D1.0, LE-B1.0D0.5, LE-B0.5D0.5, and LE-B1.0 X 0.5, respectively, compared to LE-C0 specimens. For the 28 days curing period, the compressive strengths of LY-C0 and LE-C0 specimens without fibres were 49.2 MPa and 37.5 MPa, respectively. The results showed a clear superiority of the LWAC specimens with Lytag aggregate over Leca, with an increase of 31.1%, as shown in Fig. 6(b). Group 1 specimens (with Lytag) showed a slight change, LY-B0.5D1.0 and LY-B0.5D0.5 compressive strength increased by 3% and 1.5%, respectively, while the LY-B1.0D0.5 and LY-B1.0 X 0.5 exhibited a reduction of 1.6% and 7%, respectively, compared with the LY-C0 specimens. Group 2 specimens (with Leca), showed similar trends, LE-B0.5D1.0 and LE-B0.5D0.5 showed an increased in compressive strength of 5.5% and 0.8%, respectively, while the LE-B1.0D0.5 and LE-B1.0 X 0.5 specimens exhibited a reduction of 5.7% and 30%, respectively, compared with the LE-C0 specimens. As reported in previous studies, basalt and polypropylene fibres reduce the compressive strength of lightweight concrete when used individually [54,55]. Therefore, the slight increase observed in the hybrid mix can also be explained by complementary interactions between the two fibre types.

The compressive strength of Groups 1 and 2 specimens demonstrates that the Lytag aggregate is more suitable for LWAC mixtures than the Leca aggregate (Fig. 6). The XRD patterns of the two lightweight aggregates (Fig. 7) show apparent mineralogical differences. Lytag exhibits more pronounced aluminosilicate-related peaks, indicating a denser, more sintered structure than Leca. This aligns with the higher compressive strength observed in Lytag mixes. The reduction in the compressive strength of groups 2 specimens can be attributed to the properties of Leca aggregate, which is formed from expanded clay, whereas Lytag aggregateis derived from fly ash, which contributes to enhanced compressive strength. Lytag's higher density and particle crushing resistance 11 N/mm^2 compared with 5 N/mm^2 for Leca as demonstrated in Table 2. Often provides advantage in attaining superior compressive strengths when contrasted with Leca in LWAC mixture applications. These findings align with those reported in previous investigations [56,57].

The maximum compressive strength was observed in samples containing (B0.5 +D1.0), regardless of aggregate type, which can be attributed to the improved fibre dispersion and uniform distribution of fibre within the matrix. Nonetheless, samples containing the same type (B1.0 + D0.5) and (B0.5 + D0.5) did not show a substantial increase, as illustrated in Fig. 6. However, the incorporation of BF with PPX fibres (B1.0 + X0.5) exhibited the lowest compressive strength, likely due to the poor dispersion of PPX fibres, which led to fibre agglomeration and weak interfacial bonding with the cementitious matrix [58,59]. Increasing total fibre content from 1% fibre (B0.5 + D0.5) to 1.5% fibre (B1.0 + D0.5), did not lead to substantial improvements (Fig. 6), as higher fibre content may cause poor fibre distribution, more internal defects, higher voids content and reduced overall strength [60]. Nevertheless, the inclusion of fibres improved the damage pattern of LWAC samples, allowing them to retain integrity under load rather than crumbling or falling, as shown in Fig. 8. These findings are consistent with previous studies [61,62].

The stress-strain curves of cylinder specimens at 28 days of curing are shown in Fig. 9. At the initial loading stage, the curves exhibited a uniform linear behaviour before attaining the peak compressive strength. The strains observed were quite limited during

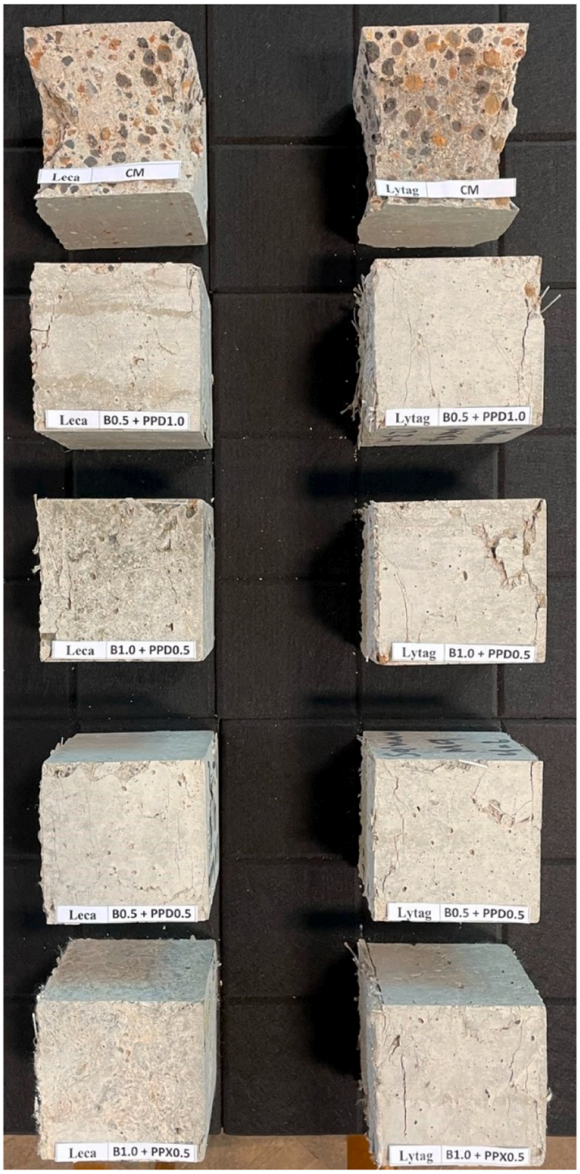

Fig. 8. Specimens after compressive strength test.

the elastic stage, as demonstrated in Fig. 9. Generally, specimens without fibre tend to fail rapidly, whereas those with fibre demonstrated greater resilience in sustaining stresses. As the load increased, the stress gradually approached its maximum values. The strains at peak stress for Lytag specimens were 0.0022, 0.0024, 0.0025, 0.0024, and 0.0025 for LY-C0, LY-B0.5D1.0, LY-B1.0D0.5, LY-B0.5D0.5, and LY-B1.0 X 0.5, respectively, as demonstrated in Fig. 9(a). For Leca specimens, the strains at peak stress were 0.0019, 0.0025, 0.0021, 0.0024, and 0.0022 for LE-C0, LE-B0.5D1.0, LE-B1.0D0.5, LE-B0.5D0.5, and LE-B1.0 X 0.5, respectively, as demonstrated in Fig. 9(b). As the stress reached its maximum, the curves started to show nonlinear behaviour, followed by gradual decline in the stress–strain curve. The capacity of the fibres to bridge cracks led to improved ductility upon attaining the peak stress, as illustrated in Fig. 9. The stress-strain curves for LWAC specimens containing fibres exhibited a more gradual decline in their stress-strain curves. Unlike the control specimens, the fibre reinforced mixture did not show a sudden drop in strength, instead they demonstrated enhanced ductility and toughness. The rise in stiffness also reflected the trend observed in compressive strength results. The LY-B0.5D1.0 and LE-B0.5D1.0 specimens exhibited the best overall performance compared with all specimens.

3.2. Bulk density

The oven-dried densities LY-C0 and LE-C0 were 1929.2 and 1754.7 kg/m^3 , respectively, these values are comparable to the findings published in [63]. According to BS EN 206 [47], LY-C0 and LE-C0 are classified as LWAC types D1.8 and D2.0, respectively.

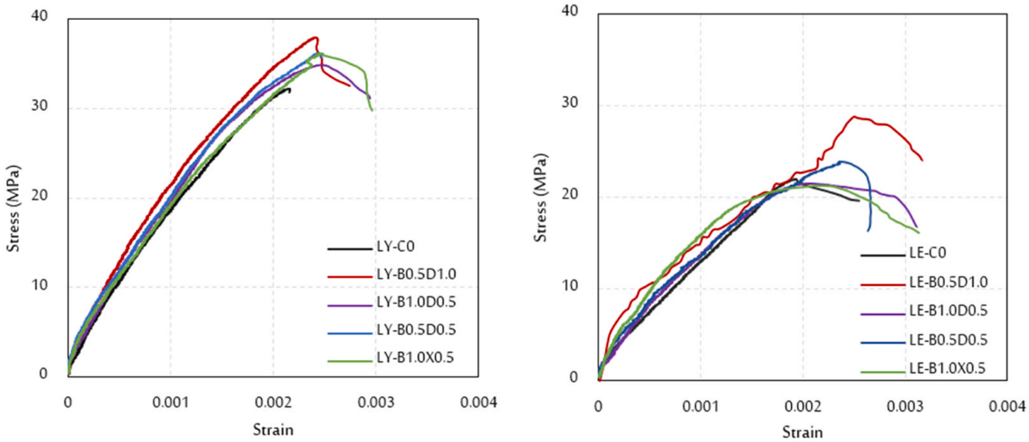

Fig. 9. Compressive stress-strain curves: (a) Lytag samples; (b) Leca samples.

Table 5
Bulk density of LWCA specimens.

Specimen ID	Aggregate Type	SSD Density (kg/m^3)	Oven Dry Density (kg/m^3)
LY-C0	Lytag	1969.8	1929.2
LY-B0.5D1.0	Lytag	1931.2	1890.6
LE-C0	Leca	1849.1	1754.7
LE-B0.5D1.0	Leca	1807.5	1701.9

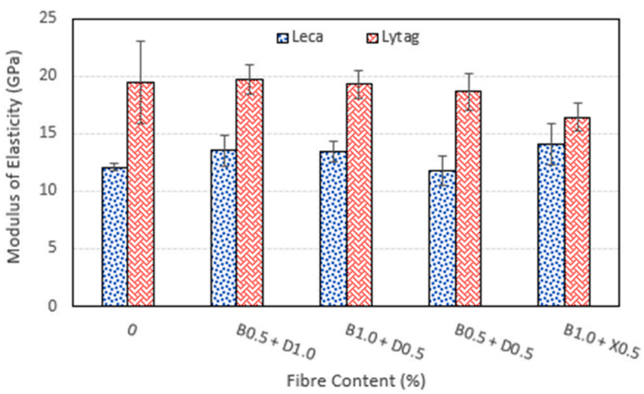

Fig. 10. Modulus of elasticity values.

This classification is based on oven-dry density, whereas both SSD and oven-dry values are reported in Table 5 for completeness. These values are also consistent with the Chinese specification [64], which sets the maximum density of LWAC at 1950 kg/m^3. The LY-B0.5D1.0 and LE-B0.5D1.0 mixtures exhibited slightly lower densities, 1890.6 and 1701.9 kg/m^3, respectively, as shown in Table 5, showing that fibre addition slightly reduces oven-dried density. This suggests that fibres contribute more to crack resistance than to the filling effects within the matrix.

3.3. Modulus of elasticity

Fig. 10 illustrates the modulus of elasticity of LWAC mixtures as ascertained from cylinder specimens at 28 days. The modulus of elasticity of LY-C0 and LE-C0 specimens was 19.49 MPa and 12.1 MPa, respectively. The results showed a clear superiority of the LWAC specimens with Lytag aggregate compared to Leca aggregate, with an increase of 61%. Generally, fibres slightly influenced the modulus of elasticity. In Group 1 (with Lytag) LY-B0.5D1.0 modulus of elasticity increased slightly by 1.1%, while LY-B1.0D0.5, LY-B0.5D0.5, and LY-B1.0 X 0.5 decreased by 1.0%, 4.1%, and 15.6%, respectively, compared with the plain specimens. In Group 2 (including Leca), LE-B0.5D1.0, LE-B1.0D0.5, and LE-B1.0 X 0.5 specimens demonstrated increases in the modulus of elasticity by

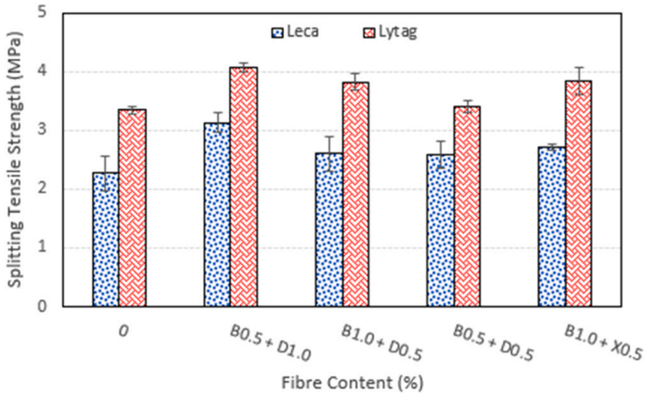

Fig. 11. Splitting tensile strength values.

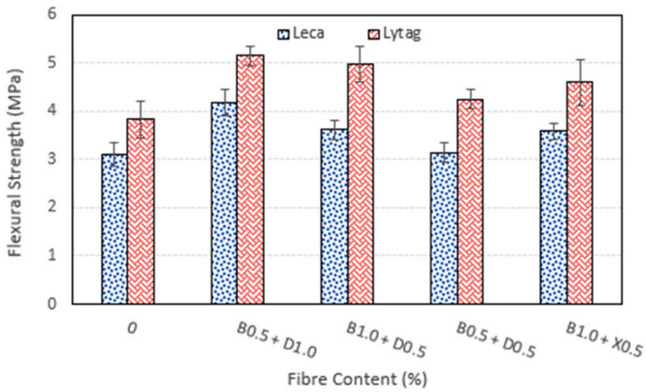

Fig. 12. Flexural strength values.

11.9%, 11.2%, and 16.1%, respectively, while LE-B0.5D0.5 specimens displayed a slight decrease of 2.7% compared to the LE-C0.

3.4. Splitting tensile strength

Fig. 11 illustrates splitting tensile strength of LWAC mixtures at 28 days. LY-C0 and LE-C0 specimens had strength of 3.35 MPa and 2.27 MPa, respectively. The results showed a clear superiority of the LWAC specimens with Lytag aggregate compared to Leca aggregate, with an increase of 47.2%. Fibres significantly improved splitting tensile strength. In Group 1 specimens (with Lytag) exhibited a significant increase in splitting tensile strength. LY-B0.5D1.0, LY-B1.0D0.5, LY-B0.5D0.5, and LY-B1.0 X 0.5 specimens showed an increased ratio of 21.6%, 14.2%, 1.7%, and 14.9%, respectively, compared with the LY-C0 specimens. For Group 2 (including Leca), LE-B0.5D1.0, LE-B1.0D0.5, LE-B0.5D0.5, and LE-B1.0 X 0.5 specimens demonstrated increases in the splitting tensile strength by 37.9%, 14.4%, 14.0%, and 19.6%, respectively, compared to the LE-C0 specimens. The highest splitting tensile strength was observed in LY-B0.5D1.0 and LE-B0.5D1.0 mixtures with 0.5% BF and 1.0% of PPD fibres.

This improvement can be attributed to the characteristics of PPD fibres', including their cross-sectional properties, elastic modulus, and tensile strength, which are superior compared to those of PPX fibres, as shown in Table 3. Therefore, combining PPD fibre with BF fibre results in a synergistic effect. The two fibres types may together influence the elastic modulus. The relatively low elastic modulus of PPD fibres helps inhibit the formation and propagation of microcracks during the early hardening phase, thereby reducing the potential crack sources. In contrast, BF fibres possess a much higher elastic modules, and their influence on crack propagation during the hardening is more pronounced. Consequently, the two fibres types can contribute at different levels to enhance the overall strength of LWAC mixtures [62,65–67]. However, the positive impact of hybrid fibre diminished as the proportion of PPD fibre decreased (from 1.0% to 0.5%). The splitting tensile strength of LWAC mixtures also declined as the proportion of BF fibre increased (from 0.5% to 1.0%). A high BF fibre content, when combined with PPD fibres, negatively impacts fibre dispersion and increased the tendency for agglomeration. This produces weak interfaces in the LWAC matrix reducing overall strength. Furthermore, the splitting tensile strength decreased when the total fibre volume dropped from 1.5% to 1.0%. The lowest splitting tensile strengths were observed in LY-B0.5D0.5 and LE-B0.5D0.5 mixtures, which contains 0.5% BF and 0.5% of PPD fibres. In addition, fibre arrangement and alignment play a critical role in determining the tensile strength of LWAC [68]. Thus, the distributions and volume fractions of fibres are crucial in achieving optimal enhancements in mechanical characteristics [63]. Evidence of a strong bond between both types of LWA and the

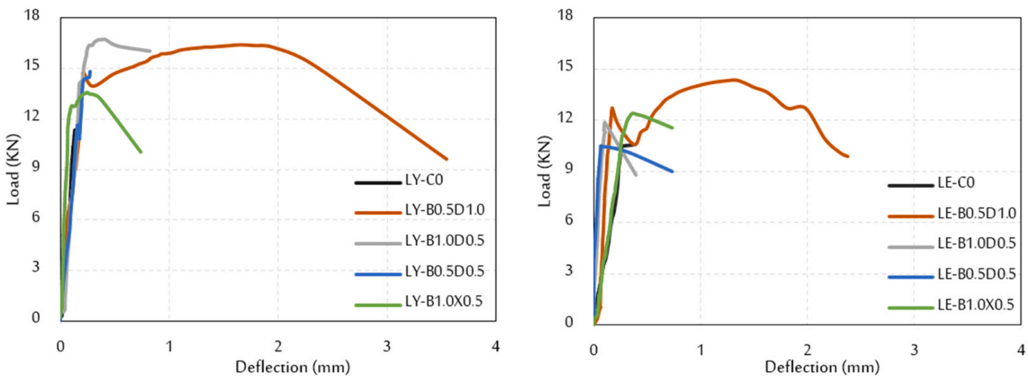

(a) (b)

Fig. 13. Load-deflection curves: (a) Lytag samples; (b) Leca samples.

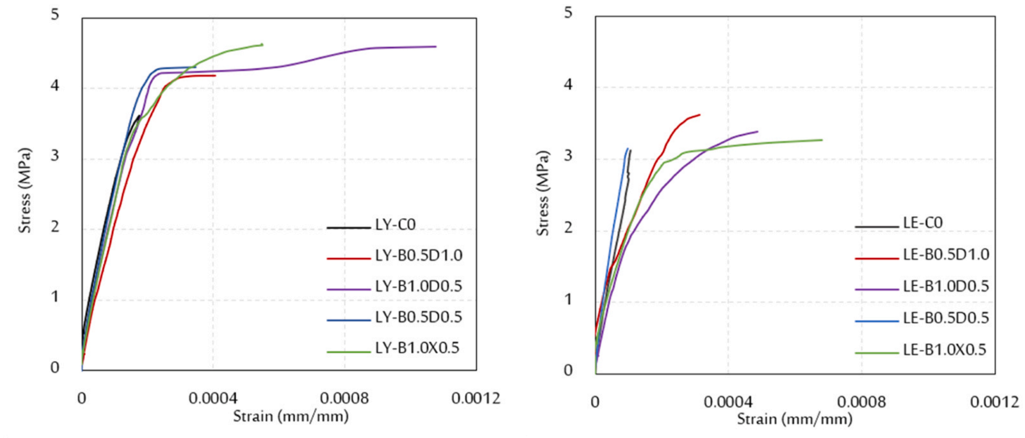

(a) (b)

Fig. 14. Strain gauge readings of the bottom concrete surface of the LWAC prism: (a) Lytag samples; (b) Leca samples.

cement matrix was confirmed by the fracture behaviour of the composite under load. Upon failure, the cracking manifested through the aggregate grains rather than at the interface between the cement matrix and the aggregate.

3.5. Flexural strength characterization

3.5.1. Flexural strength

Fig. 12 illustrates the flexural strength of LWAC mixtures obtained from prism specimens at 28 days. The flexural strengths of LY-C0 and LE-C0 specimens without fibres were 3.84 MPa and 3.10 MPa, respectively. The results demonstrated a distinct advantage of Lytag aggregate over Leca, with an enhancement of 23.6%. As shown in Fig. 12 the addition of various fibre types results in varying levels of enhancement in flexural strength. Group 1 specimens (including Lytag) exhibited significant increases in flexural strength. LY-B0.5D1.0, LY-B1.0D0.5, LY-B0.5D0.5, and LY-B1.0 X 0.5 improved by 34.2%, 29.6%, 10.9%, and 19.8%, respectively, compared with LY-C0 specimens. Group 2 specimens (including Leca) also improved, LE-B0.5D1.0, LE-B1.0D0.5, LE-B0.5D0.5, and LE-B1.0 X 0.5 specimens demonstrated increases of 34.3%, 16.4%, 1.4%, and 15.9%, respectively, compared with LE-C0. The maximum flexural strength was observed in LY-B0.5D1.0 and LE-B0.5D1.0 mixtures reinforced with 0.5% BF and 1.0% of PPD fibres. This combination promoted uniform fibre distribution within the LWAC Matrix. Similar to the tensile strength, the improvement in flexural strength can be attributed to the superior characteristics of the PPD fibres, in comparison to PPX fibres, as demonstrated in Table 3. Consequently, combining PPD fibre and BF fibre produce a synergistic effect. The positive influence of hybrid fibres diminished as the PPD fibre

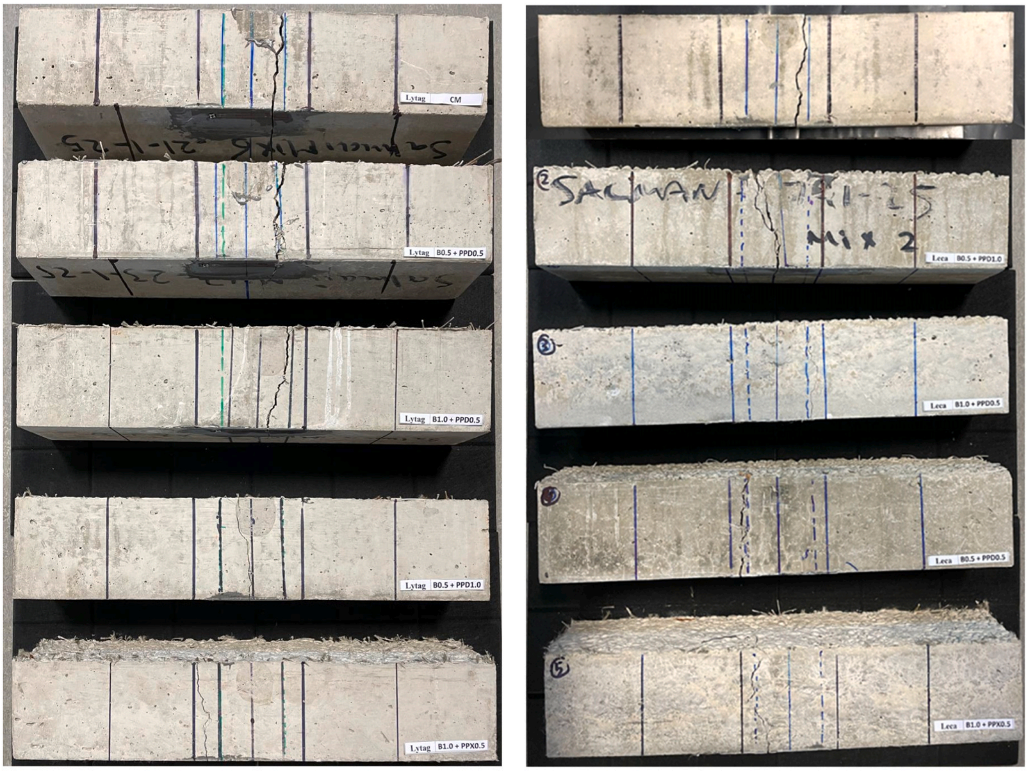

(a) (b)

Fig. 15. Failure modes: (a) Lytag samples; (b) Leca samples.

proportion decreased (from 1.0% to 0.5%). Likewise, flexural strength generally declined when the BF content increased (from 0.5% to 1.0%), indicating that the contribution of PPD fibre to flexural strength is greater than that of the BF or PPX fibres. A higher proportion of BF when combined with PPD fibre, led to poor dispersion, fibre agglomeration and weak interfaces in the LWAC mixture, thereby reducing strength. In contrast, increasing the overall fibre volume fraction (from 1.0 to 1.5%) resulted in further gains in flexural strength.

3.5.2. Load–deflection behaviour

Fig. 13 illustrates the load-deflection behaviour of LWAC prisms. All mixture began with a linear elastic phase, which steeply linearised up to their peak load, after which the slope decreased due to concrete cracking, leading to a nonlinear response. A clear distinction emerged after a small deflection. Control specimens without fibres (LY-C0 and LE-C0) exhibited a sudden drop in load after reaching their peak values, (13.27 kN for LY-C0 at 0.189 mm and 10.56 kN LE-C0 at 0.366 mm), followed by brittle failure as shown in Fig. 13. In contrast, fibre reinforced specimens display improved flexural strength and deformation capacity, with noticeable deflection-hardening behaviour. Increase the fibre volume fraction enhanced load-carrying capacity, as fibres restricted crack growth and delayed failure. However, once the applied stress exceeded the fibre -matrix bond strength, fibres were pulled out, reducing reinforcement efficiency. For Group 1, the first peak loads of 14.73 kN, 16.73 kN, 14.84 kN, and 13.55 kN for LY-B0.5D1.0, LY-B1.0D0.5, LY-B0.5D0.5, and LY-B1.0 X 0.5 at deflections of 0.216 mm, 0.388 mm, 0.275 mm, and 0.253 mm, respectively. For Group 2 the corresponding values were 12.71 kN, 11.88 kN, 10.52 kN, and 12.39 kN for LE-B0.5D1.0, LE-B1.0D0.5, LE-B0.5D0.5, and LE-B1.0 X 0.5 at deflections of 0.176 mm, 0.107 mm, 0.069 mm, and 0.367 mm, respectively. Overall, Lytag mixture outperformed Leca mixtures, as illustrated in Fig. 13. The best performance was observed in LY-B0.5D1.0 and LE-B0.5D1.0, which failed at much larger deflection of 3.548 mm and 2.375 mm, respectively. Regardless of aggregate type mixture with B1.0 + D0.5, B0.5 + D0.5, and B1.0 + X0.5 fibres showed deflection-hardening characteristics after initial cracking, but lost load capacity rapidly at small deflections (less than 1 mm). By contrast, mixture with 0.5% of BF + 1.0% of PPD sustained deflection-hardening behaviour well beyond peak load, demonstrating superior ductility compared with other hybrid fibre combinations.

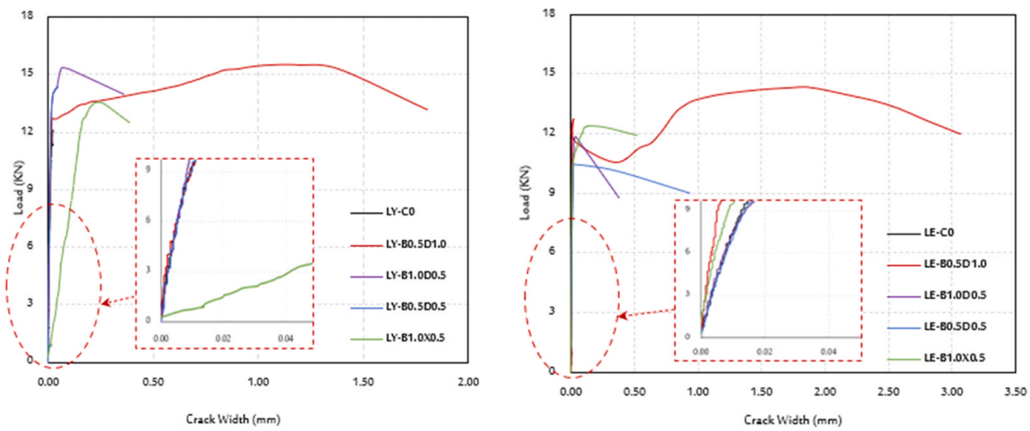

(a) (b)

Fig. 16. Crack width of the LWAC prism: (a) Lytag samples; (b) Leca samples.

Fig. 14 presents the tensile strain at the bottom surface of the prisms, highlighting the maximum readings recorded prior to the fracture of the gauges. The tensile strain patterns were symmetrical in early loading stages with high stress accompanied by low tensile strain. Cracking near the midspan region, where strain gauges were positioned, caused some local variations. Fibre -reinforced specimens showed higher tensile strains than the controls (LY-C0 and LE-C0), confirming that fibre inclusion increased deformation capacity. The load-deformation curves support this finding, demonstrating that the fibre-reinforced LWAC specimens sustained significantly larger deformations prior to failure.

3.5.3. Failure modes of LWAC prism

Fig. 15 illustrates the failure modes of all the LWAC prisms. The LY-C0 and LE-C0 specimens exhibited brittle failure, characterized by a single crack in the pure bending region, which caused the specimens to fracture into two distinct blocks, as shown in Fig. 15. The other LWAC prisms experienced ductile failure, distinguished by thinner crack propagation, attributed to the bridging effect of the fibres. Regardless of the LWA and fibre types, a single crack was noticed in the prism's midspan. Once cracking initiated in the LWAC matrix, the tensile force resisted by the fibres was progressively transferred to the surrounding matrix on either side of the crack through interface bonding [69].

As the crack width or transmission distance increased beyond critical length, the LWAC matrix developed additional cracking. The fibres, however, restricted further crack growth, slowed its propagation, delayed specimen failure, and enhanced both tensile strength and toughness. When the tensile stress exceeded the bond strength between the LWAC matrix and the fibres, fibre pull-out occurred, leading to loss of reinforcement effectiveness. In this study, the maximum crack width at the midspan of the LWAC prism in the bending moment region was measured using an LVDT crack opening displacement sensor. Table 6 presents the maximum crack widths recorded immediately before the LVDT detached from the concrete surface.

Fig. 16 shows the load-crack width plots. For all tested LWAC prisms, once the initial cracking load was reached, vertical cracks appeared in the pure bending region, and their widths continued to grow as the applied load increased. Due to the sudden brittle failure of the control specimens, the LVDT could not capture the crack measurements at the point of complete fracture; consequently, the LVDT detached from the concrete surface at a crack width of 0.02 mm for both LY-C0 and LE-C0 specimens, as reported in Table 6. For Group 1 specimens, the maximum crack widths were 1.81 mm, 0.36 mm, 0.05 mm, and 0.39 mm for LY-B0.5D1.0, LY-B1.0D0.5, LY-B0.5D0.5, and LY-B1.0 X 0.5, respectively. For Group 2 specimens, the corresponding maximum crack widths obtained were 3.07 mm, 0.38 mm, 0.95 mm, and 0.52 mm for LE-B0.5D1.0, LE-B1.0D0.5, LE-B0.5D0.5, and LE-B1.0 X 0.5, respectively. These results confirms that the incorporation of fibres effectively mitigated the rapid propagation of cracks.

3.5.4. Fracture toughness

The capacity of material to absorb energy is related to the flexural toughness of the LWAC prism, which is quantified by the area under the load-deflection curve up to a specified deflection point. The ASTM C1609 [70] method, an advancement of the ASTM C1018 [71] method, was employed in this study to overcome the challenge of identifying the first crack point. This approach yields equivalent flexural strength ($f^D_{e,600}$) and the equivalent flexural toughness ratio ($R^D_{T,600}$) of fibre-reinforced concrete, as expressed in Eqs. 1 and 2:

$$f^D_{e,600} = \frac{150 \quad T^D_{600}}{b\, d^2} \tag{1}$$

Table 6
Flexural toughness of LWAC mixtures.

Specimen ID	Crack width (mm)	T^D_{600} (N·mm)	T^D_{total} (N·mm)	$f^D_{e,600}$ (MPa)	$R^D_{T,600}$
LY-C0	0.02	-	1323.10	-	-
LY-B0.5D1.0	1.81	7007.23	49854.62	1.05	0.204
LY-B1.0D0.5	0.36	6668.82	11495.66	1.00	0.201
LY-B0.5D0.5	0.05	2439.74	2439.74	0.37	0.086
LY-B1.0 × 0.5	0.39	4195.26	8566.96	0.63	0.137
LE-C0	0.02	-	2383.10	-	-
LE-B0.5D1.0	3.07	4926.18	29013.42	0.74	0.177
LE-B1.0D0.5	0.38	3718.69	3718.69	0.56	0.154
LE-B0.5D0.5	0.95	3250.99	7012.05	0.49	0.155
LE-B1.0 × 0.5	0.52	4138.42	6958.13	0.62	0.173

$$R^D_{T,600} = \frac{150 \quad T^D_{600}}{f_1 \; b \; d^2} x \quad 100\% \tag{2}$$

, where T^D_{600} refers to the area under the load-deflection curve up to a deflection of L/600 (N.mm), f_1 refers to first-peak strength (MPa), b refers to prism width (mm), and d refers to prism height (mm).

Flexural toughness indices were obtained from the load-deflection curves at net deflections of $L/150$ and $L/600$ of the span length. However, for most LWAC prisms tested in this study, the peak deflections did not exceed $L/150 = 2mm$. In addition, the total area enclosed (T^D_{total}, energy absorbed) under the curves was calculated to further illustrate the contributions of fibres to fracture performance of LWAC prisms. The results in Table 6 provide fracture toughness as per ASTM C1609. The findings distinctly demonstrate that the energy absorption capacity (T^D_{total}) of the LWAC prism incorporating fibres surpasses that of those without fibres. The maximum T^D_{total} were observed in LY-B0.5D1.0 and LE-B0.5D1.0 mixtures, which contained 0.5% BF and 1.0% of PPD fibres. LWAC specimens made with Lytag aggregate exhibited superior fracture toughness compared to those with Leca aggregate, showing an increase of 71.8%. Furthermore, the T^D_{total} diminished when the fibre volume decreased from 1.5% to 1.0%. Similar trend observed in the equivalent flexural toughness ratio ($R^D_{T,600}$). The highest $R^D_{T,600}$ again recorded in LY-B0.5D1.0 and LE-B0.5D1.0 combinations. The findings demonstrated a distinct advantage of the LWAC specimens utilising Lytag aggregate over those with Leca aggregate, exhibiting a 15.2% rise, as illustrated in Table 6. Moreover, $R^D_{T,600}$ decreased as the fibre volume reduced from 1.5% to 1.0%. Although the inclusion of PPX fibres in LWAC mixtures adversely affected compressive strength, they demonstrated satisfactory performance in flexural resistance, as illustrated in Fig. 13 and Table 6.

4. Microstructure analysis

4.1. SEM analysis

Fig. 17 illustrates the morphology of the microstructure of LWAC mixtures. The SEM image offers a microstructural view of BF and PPD fibres embedded in the LWAC matrix. It emphasizes the fibre-matrix interface interaction, the porous character of the concrete, and the morphology of the fibres. As is typical of lightweight concrete, the surrounding material has an uneven, rough, and porous texture. Within the cementitious matrix, voids and sharp aggregate particles are visible, as shown in Fig. 17. The BF fibre is visible as a collection of long, cylindrical structures that run through the concrete matrix, as shown in Fig. 17(a). PPD fibres are recognizable, elongated features that were seen to run across the surface. In contrast to the rougher concrete matrix, they have a somewhat smooth and cylindrical appearance, as shown in Fig. 17(b). The measured ITZ was noticeably thinner around basalt fibres (0.5–2 μm) than around polypropylene fibres (2–4 μm). Similar trends have been reported in the literature, in which basalt fibres form a denser and stronger ITZ than polypropylene fibres, supporting the stronger bonding trend observed in mixes [72].

4.2. EDAX analysis

Fig. 18 illustrates EDAX analysis of BF and PPD fibres. EDAX analysis shows the elemental composition of the examined sample by means of a spectrum and an elemental composition chart. The height and area of each peak are proportional to the concentration of that element. EDAX analysis shows the fundamental components of the examined area with BF in lightweight concrete, as shown in Fig. 18(a). It emphasizes the notable abundance of oxygen, silicon, and aluminum, as well as other elements typical of the BF fibres. The information reveals the chemical composition of the BF at the microstructural level, therefore supporting its low carbon footprint and other environmentally beneficial qualities. Fig. 18(b) shows that the most prominent peak in the EDAX analysis of PPD fibres is clearly labeled Calcium (Ca). The bar chart clearly shows that Ca is the most abundant element by weight. This implies that the PPD is mostly made up of a calcium-rich compound, with many other elements present in far lower weight proportions. This is very different from the expected composition of pure polypropylene, therefore supporting its low carbon footprint and other environmentally beneficial qualities.

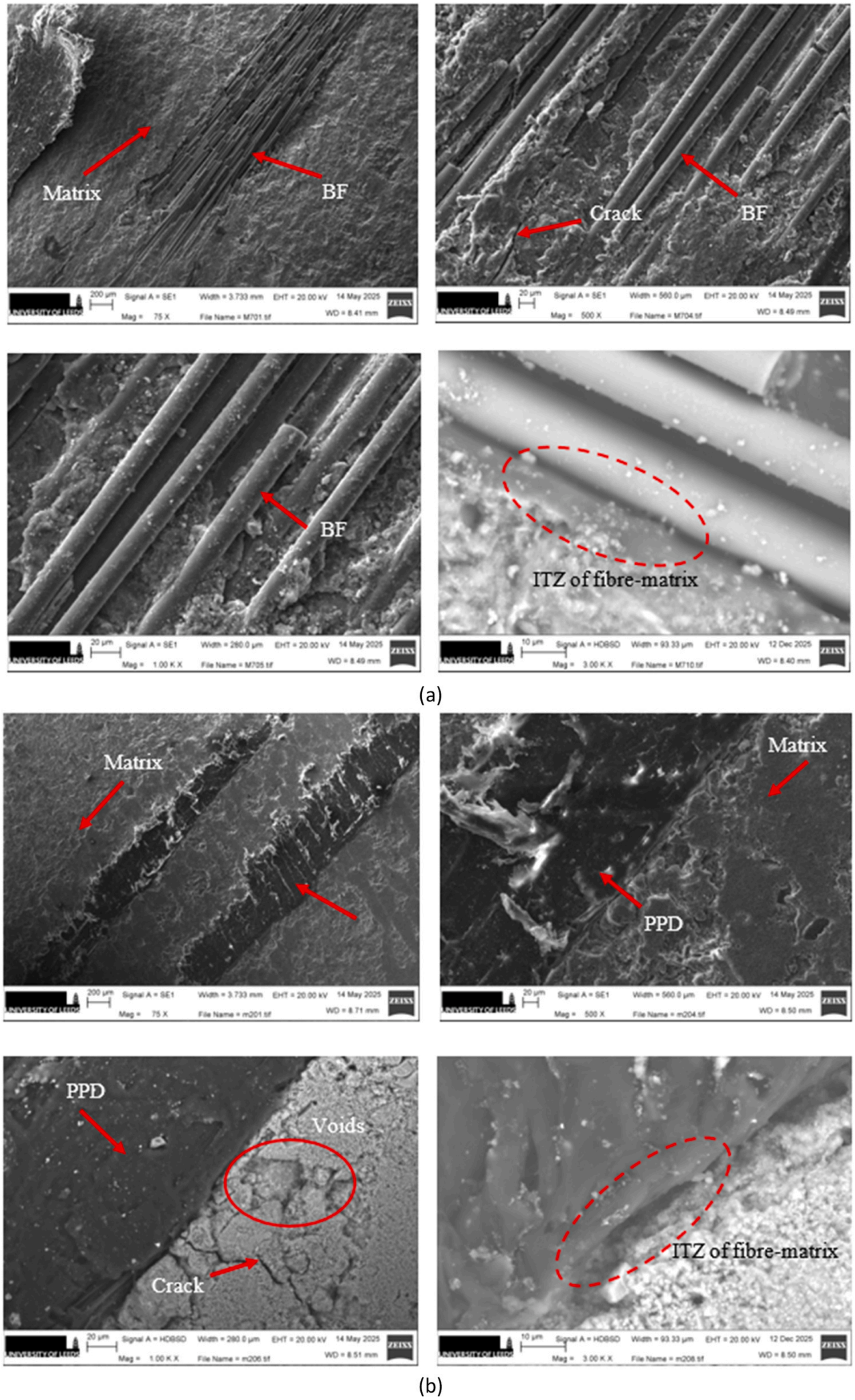

Fig. 17. SEM micrographs: (a) BF; (b) PPD.

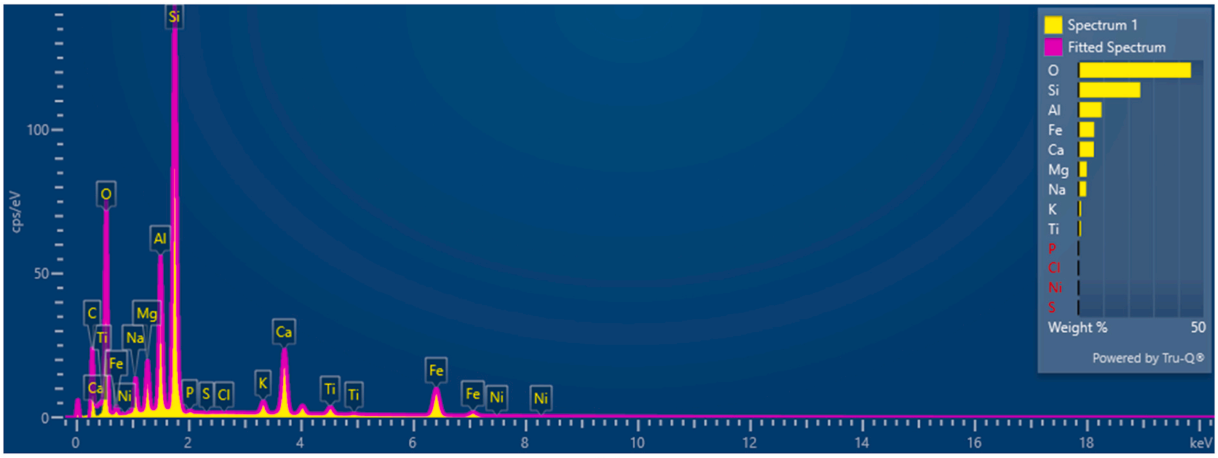

(a)

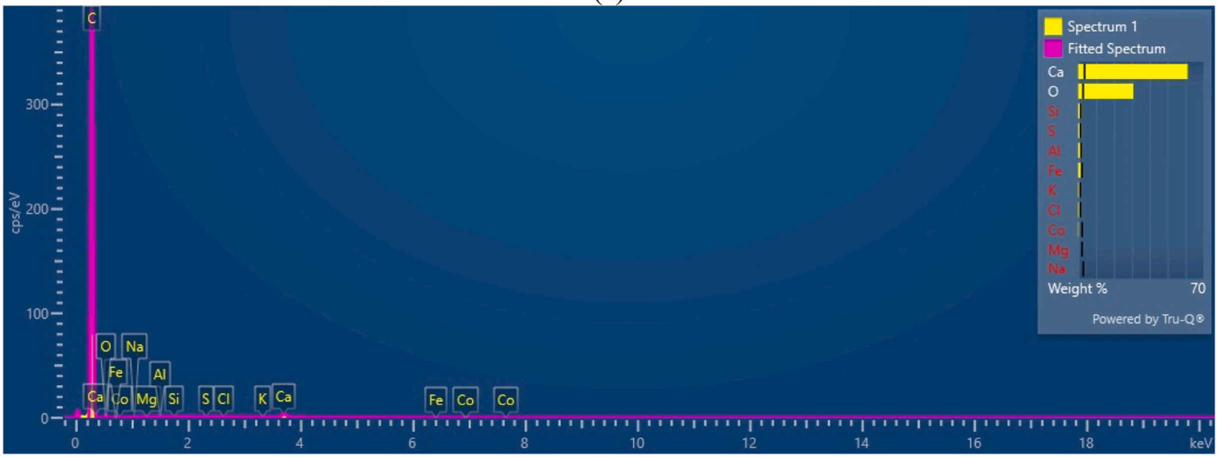

(b)

Fig. 18. EDAX analysis: (a) BF; (b) PPD.

4.3. Image analysis using Fiji

Image analysis was conducted using Fiji (Fiji is just ImageJ), version 2.14.0, running on Java 1.8.0_322 (64-bit). Each selected ROI (90 × 40 mm) for the horizontal section and (90 × 90 mm) for the vertical section was first converted to 8-bit grayscale. Vertical and horizontal measurement lines were selected at the mid-depth of the specimen. A fixed image resolution (3 pixels = 1 mm) was maintained across all samples to ensure consistent spatial representation. Segmentation of the concrete phases was performed using manual thresholding based on grayscale intensity ranges, determined experimentally for each constituent. Each phase was isolated separately using threshold-based masking. The area fraction (%) of each phase within the ROI was calculated using the Measure function in Fiji, with the "Limit to Threshold" option enabled and edge regions excluded to reduce measurement artifacts. Fig. 19(a-f) show an example of image analysis using Fiji for the LE-B0.5D1.0 sample. Table 7 displays the components of the LWAC specimens as determined by the image analysis results. Image analysis indicates that specimens containing Leca aggregate display a greater surface aggregate content in the horizontal section compared to those with Lytag aggregate. The LWA content in the LE-C0 and LY-C0 was 62.22% and 33.09%, respectively, with an increased ratio of 88.0% for LE-C0 compared with LY-C0 specimens. The same trend was noticed in the specimens with fibres, where LE-B0.5D1.0 shows an increased ratio of 53.2% of LWA compared with LY-B0.5D1.0 specimens. The lower density of Leca aggregate results in a higher percentage floating on the surface of the samples when compared to Lytag aggregate. This phenomenon accounts for the reduced compressive strength observed in these samples. The results demonstrated that the incorporation of fibre in the specimens resulted in greater void volumes in the vertical section compared to the control specimens. The voids in the vertical section of the LE-B0.5D1.0 and LY-B0.5D1.0 specimens increased by amounts of 10 and 5.5 times, respectively, compared to LE-C0 and LY-C0. This phenomenon explains the lack of enhancement in compressive strength due to the incorporation of fibres into the specimens, as discussed in Section 3.1. For completeness, Fig. 19(g) shows the worst-performing mix, in which localised PPX fibre agglomeration is clearly visible. This clustering reduced the fibres' effectiveness, contributing to the observed loss in compressive strength.

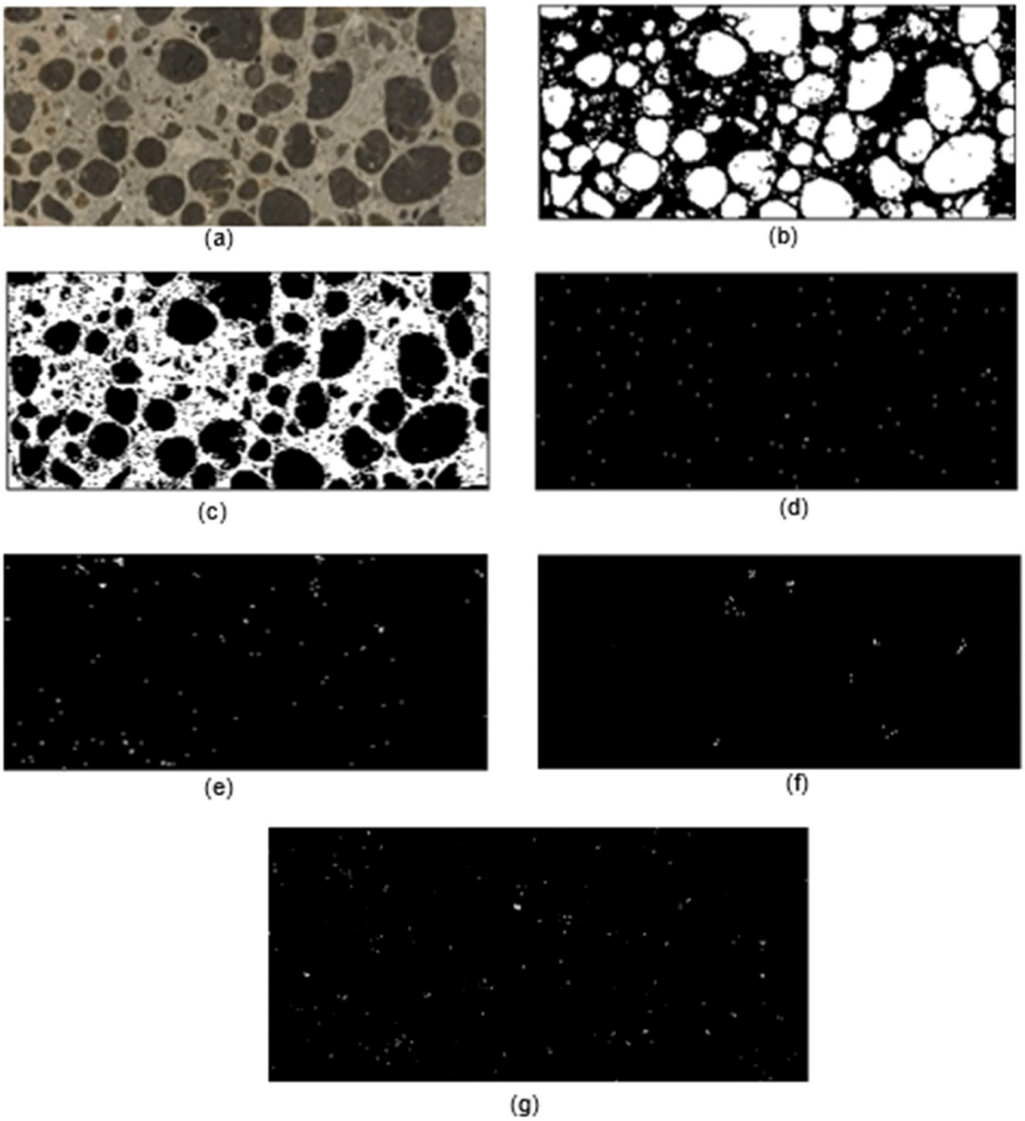

Fig. 19. An example of image analysis using Fiji for the LE-B0.5D1.0 sample: (a) Original top image; (b) Aggregates; (c) Cement matrix; (d) BF; (e) PPD; (f) Voids; (g) PPX.

Table 7
The image analysis results.

Specimen ID	Section	Aggregates (%)	Cement matrix (%)	BF (%)	PPD (%)	Voids (%)	Residual (Unaccounted) (%)
LY-C0	Horizontal	33.09	65.31	0	0	0.28	1.32
	Vertical	34.50	64.71	0	0	0.12	0.67
LY-B0.5D1.0	Horizontal	25.23	59.69	2.34	11.29	0.23	1.22
	Vertical	30.08	59.06	1.42	6.81	0.66	1.97
LE-C0	Horizontal	62.22	36.98	0	0	0.32	0.48
	Vertical	51.55	47.53	0	0	0.06	0.86
LE-B0.5D1.0	Horizontal	48.93	45.08	2.18	2.96	0.84	0.01
	Vertical	43.35	50.95	3.22	1.86	0.60	0.02

5. Conclusion

This research investigated the mechanical properties of lightweight aggregate concrete reinforced with hybrid fibres (polypropylene and basalt fibres) and incorporating two lightweight aggregates (Lytag and Leca). The main conclusions drawn are as follows:

1. Lytag-based LWAC consistently overperformed Leca-based LWAC, exhibiting enhancements in compressive strength, modulus of elasticity, splitting tensile strength, and flexural strength of 31.1%, 61%, 47.2%, and 23.6%, respectively. This is attributed to the higher density and crushing resistance of Lytag compared with Leca.
2. Fibres additions had only a minor effect on compressive strength, with slight increases in Lytag mixtures up to 5.5% and reductions in Leca mixtures of up to 30%. A similar trend was observed for the modulus of elasticity.
3. Splitting tensile and flexural strength were significantly enhanced by fibres, with increases of up to 37.9% and 34.3% for Lytag and Leca mixtures, respectively. The best performance was achieved with 0.5%BF+ 1.0%PPD, regardless of aggregate type.
4. Mixtures with PPX fibres combined with BF performed the weakest in compressive strength, with a reduction of 30% compared to the control mixture, although they showed acceptable flexural resistance (with an increase of up to 19.8% compared to the control mixture).
5. Hybrid fibres improved failure mode, which can ensure that the fibre-reinforced LWAC mixture maintains its integrity under stress without crumbling or falling, resulting in a favourable damage pattern. Meanwhile, the fracture behaviour of the LWAC specimens under load indicates a robust adhesion between the LWA and the cement matrix, with breaking predominantly occurring within the LWA grains rather than at the cement matrix interface.
6. Energy absorption capacity was improved by fibres. The same trend was noticed for the equivalent flexural toughness ratio ($R^D_{T,600}$). The highest $R^D_{T,600}$ was recorded in the LY-B0.5D1.0 and LE-B0.5D1.0 combinations.
7. Overall, a recommendation is to use 1.5% volume fractions of both BF (0.5%) and PPD (1.0%) in LWAC to achieve the most significant enhancement in mechanical properties, providing the best balance of strength, ductility, and fracture resistance.
8. Further comprehensive investigations to explore the rheology and segregation of LWAC mixtures. Additionally, the long-term strength development, post-cracking behaviour under sustained loads, and residual mechanical properties after high-temperature exposure should be investigated.

CRediT authorship contribution statement

Suhaila Mattar: Writing – review & editing, Validation, Supervision, Conceptualization. **Aref A. Abadel:** Writing – review & editing, Formal analysis. **Salman Alnasser:** Writing – review & editing, Writing – original draft, Visualization, Software, Methodology, Investigation, Formal analysis, Data curation, Conceptualization.

Declaration of Competing Interest

The authors declare that they have no known competing financial interests or personal relationships that could have appeared to influence the work reported in this paper.

Acknowledgments

The author acknowledges the guidance of Prof. Emilio Garcia-Taengua during this research. They also wish to express, with all sincerity, their appreciation to the Saudi Arabian Cultural Mission in the United Kingdom (SACM-UK) for its continuous encouragement of academic research. The word of special thanks goes to the laboratory technicians for their valuable assistance during the experimental work.

Data availability

Data will be made available on request.

References

[1] M.H. Zhang, O.E. Gjvorv, Mechanical properties of high-strength lightweight concrete, Mater. J. 88 (3) (1991) 240–247, https://doi.org/10.14359/1839.
[2] W.H. Juimo Tchamdjou, T. Cherradi, M.L. Abidi, L.A. Pereira-de-Oliveira, Mechanical properties of lightweight aggregates concrete made with cameroonian volcanic scoria: destructive and non-destructive characterization, J. Build. Eng. 16 (2018) 134–145, https://doi.org/10.1016/j.jobe.2018.01.003.
[3] A. Wongkvanklom, P. Posi, B. Khotsopha, C. Ketmala, N. Pluemsud, S. Lertnimoolchai, P. Chindaprasirt, Structural lightweight concrete containing recycled lightweight concrete aggregate, KSCE J. Civ. Eng. 22 (2018) 3077–3084, https://doi.org/10.1007/s12205-017-0612-z.
[4] M. Aslam, P. Shafigh, M. Alizadeh Nomeli, M. Zamin Jumaat, Manufacturing of high-strength lightweight aggregate concrete using blended coarse lightweight aggregates, J. Build. Eng. 13 (2017) 53–62, https://doi.org/10.1016/j.jobe.2017.07.002.
[5] T.Y. Lo, W.C. Tang, H.Z. Cui, The effects of aggregate properties on lightweight concrete, Build. Environ. 42 (2007) 3025–3029, https://doi.org/10.1016/j.buildenv.2005.06.031.
[6] R. Polat, R. Demirboğa, M.B. Karakoç, İ. Türkmen, The influence of lightweight aggregate on the physico-mechanical properties of concrete exposed to freeze–thaw cycles, Cold Reg. Sci. Technol. 60 (2010) 51–56, https://doi.org/10.1016/j.coldregions.2009.08.010.

[7] H. Al-Khaiat, M.N. Haque, Effect of initial curing on early strength and physical properties of a lightweight concrete, Cem. Concr. Res 28 (1998) 859–866, https://doi.org/10.1016/s0008-8846(98)00051-9.
[8] K.M.A. Hossain, S. Ahmed, M. Lachemi, Lightweight concrete incorporating pumice based blended cement and aggregate: mechanical and durability characteristics, Constr. Build. Mater. 25 (2011) 1186–1195, https://doi.org/10.1016/j.conbuildmat.2010.09.036.
[9] K.M.A. Hossain, Properties of volcanic scoria based lightweight concrete, Mag. Concr. Res. 56 (2004) 111–120, https://doi.org/10.1680/macr.56.2.111.36296.
[10] K. Kohno, T. Okamoto, Y. Isikawa, T. Sibata, H. Mori, Effects of artificial lightweight aggregate on autogenous shrinkage of concrete, Cem. Concr. Res 29 (1999) 611–614, https://doi.org/10.1016/s0008-8846(98)00202-6.
[11] S. Xu, K. Yan, T. Jiang, Y. Wang, S. Shi, W. Li, Y. Zhao, K. Sun, J. Yu, X. Wu, Compressive properties of basalt fibers and polypropylene fiber-reinforced lightweight concrete, ACS Omega 9 (2024) 26973–26982.
[12] C. Jiang, K. Fan, F. Wu, D. Chen, Experimental study on the mechanical properties and microstructure of chopped basalt fibre reinforced concrete, Mater. amp Des. 58 (2014) 187–193, https://doi.org/10.1016/j.matdes.2014.01.056.
[13] H. Ghasemzadeh Mosavinejad, A. Saradar, B. Tahmouresi, Hoop stress-strain in fiber-reinforced cementitious composite thin-walled cylindrical shells, J. Mater. Civ. Eng. 30 (2018), https://doi.org/10.1061/(asce)mt.1943-5533.0002428.
[14] J. Gao, W. Sun, K. Morino, Mechanical properties of steel fiber-reinforced, high-strength, lightweight concrete, Cem. Concr. Compos. 19 (1997) 307–313, https://doi.org/10.1016/s0958-9465(97)00023-1.
[15] A. Sadrmomtazi, B. Tahmouresi, A. Saradar, Effects of silica fume on mechanical strength and microstructure of basalt fiber reinforced cementitious composites (BFRCC), Constr. Build. Mater. 162 (2018) 321–333, https://doi.org/10.1016/j.conbuildmat.2017.11.159.
[16] O. Kayali, M.N. Haque, B. Zhu, Some characteristics of high strength fiber reinforced lightweight aggregate concrete, Cem. Concr. Compos 25 (2003) 207–213, https://doi.org/10.1016/s0958-9465(02)00016-1.
[17] V. Corinaldesi, G. Moriconi, Use of synthetic fibers in self-compacting lightweight aggregate concretes, J. Build. Eng. 4 (2015) 247–254, https://doi.org/10.1016/j.jobe.2015.10.006.
[18] M. Hassanpour, P. Shafigh, H.Bin Mahmud, Lightweight aggregate concrete fiber reinforcement – a review, Constr. Build. Mater. 37 (2012) 452–461, https://doi.org/10.1016/j.conbuildmat.2012.07.071.
[19] S.M. Abtahi, M. Sheikhzadeh, S.M. Hejazi, Fiber-reinforced asphalt-concrete – a review, Constr. Build. Mater. 24 (2010) 871–877, https://doi.org/10.1016/j.conbuildmat.2009.11.009.
[20] A. Mansoori, M.M. Moein, E. Mohseni, Effect of micro silica on fiber-reinforced self-compacting composites containing ceramic waste, J. Compos Mater. 55 (2020) 95–107, https://doi.org/10.1177/0021998320944570.
[21] R. Ralegaonkar, H. Gavali, P. Aswath, S. Abolmaali, Application of chopped basalt fibers in reinforced mortar: a review, Constr. Build. Mater. 164 (2018) 589–602, https://doi.org/10.1016/j.conbuildmat.2017.12.245.
[22] L.T. Loh, M.K. Yew, M.C. Yew, J.H. Beh, F.W. Lee, S.K. Lim, K.Z. Kwong, Mechanical and thermal properties of synthetic polypropylene fiber–reinforced renewable oil palm shell lightweight concrete, Materials 14 (2021) 2337.
[23] A. Hosseini Mehrab, S. Amirfakhrian, M.R. Esfahani, Fracture characteristics of various concrete composites containing polypropylene fibers through five fracture mechanics methods, Mater. Test. 65 (2023) 10–32.
[24] R.F. Zollo, Fiber-reinforced concrete: an overview after 30 years of development, Cem. Concr. Compos 19 (1997) 107–122, https://doi.org/10.1016/s0958-9465(96)00046-7.
[25] X. Wang, J. He, A.S. Mosallam, C. Li, H. Xin, The effects of fiber length and volume on material properties and crack resistance of basalt fiber reinforced concrete (BFRC), Adv. Mater. Sci. Eng. 2019 (2019) 1–17, https://doi.org/10.1155/2019/7520549.
[26] M. Nili, V. Afroughsabet, Combined effect of silica fume and steel fibers on the impact resistance and mechanical properties of concrete, Int J. Impact Eng. 37 (2010) 879–886, https://doi.org/10.1016/j.ijimpeng.2010.03.004.
[27] W. Yao, J. Li, K. Wu, Mechanical properties of hybrid fiber-reinforced concrete at low fiber volume fraction, Cem. Concr. Res 33 (2003) 27–30.
[28] K.H. Yang, Tests on concrete reinforced with hybrid or monolithic steel and polyvinyl alcohol fibers, Acids Mater. J. 108 (2011).
[29] E.A.H. Alwesabi, B.H.A. Bakar, I.M.H. Alshaikh, H.M. Akil, Experimental investigation on mechanical properties of plain and rubberised concretes with steel–polypropylene hybrid fibre, Constr. Build. Mater. 233 (2020) 117194.
[30] R. Madandoust, M. Kazemi, P.K. Talebi, J. de Brito, Effect of the curing type on the mechanical properties of lightweight concrete with polypropylene and steel fibres, Constr. Build. Mater. 223 (2019) 1038–1052, https://doi.org/10.1016/j.conbuildmat.2019.08.006.
[31] J. Li, C. Wan, X. Zhang, J. Niu, Fracture property of polypropylene fibre-reinforced lightweight concrete at high temperatures, Mag. Concr. Res. 72 (2020) 1147–1154, https://doi.org/10.1680/jmacr.17.00432.
[32] E.G. Badogiannis, KI. Christidis, G.E. Tzanetatos, Evaluation of the mechanical behavior of pumice lightweight concrete reinforced with steel and polypropylene fibers, Constr. Build. Mater. 196 (2019) 443–456, https://doi.org/10.1016/j.conbuildmat.2018.11.109.
[33] N.A. Libre, M. Shekarchi, M. Mahoutian, P. Soroushian, Mechanical properties of hybrid fiber reinforced lightweight aggregate concrete made with natural pumice, Constr. Build. Mater. 25 (2011) 2458–2464, https://doi.org/10.1016/j.conbuildmat.2010.11.058.
[34] J. Zhao, Y. Liu, W. Liu, J. Lin, Z. Lu, Y. Feng, J. Xie, Lightweight ultra-high performance concrete with waste glass powder: mixing proportioning design, mechanical properties and microstructure, J. Build. Eng. 112 (2025) 113662, https://doi.org/10.1016/j.jobe.2025.113662.
[35] B. Zhang, Y. Feng, J. Xie, J. He, T. Yu, C. Cai, D. Huang, Compressive behaviours, splitting properties, and workability of lightweight cement concrete: the role of fibres, Constr. Build. Mater. 320 (2022) 126237, https://doi.org/10.1016/j.conbuildmat.2021.126237.
[36] F. Chen, J. Zhao, H. Zhong, Y. Feng, C. Chen, J. Xie, An investigation of the durability of ultra-lightweight high-strength geopolymeric composites, J. Build. Eng. 80 (2023) 107990, https://doi.org/10.1016/j.jobe.2023.107990.
[37] F. Chen, J. Zhao, B. Zhang, Y. Feng, C. Chen, Z. Lu, J. Yang, J. Xie, Physical, mechanical and microstructural properties of ultra-lightweight high-strength geopolymeric composites, Case Stud. Constr. Mater. 19 (2023) e02446, https://doi.org/10.1016/j.cscm.2023.e02446.
[38] B. Zhang, Y. Feng, J. Xie, J. He, Y. Zhang, C. Cai, D. Huang, L. Li, Effects of fibres on ultra-lightweight high strength concrete: dynamic behaviour and microstructures, Cem. Concr. Compos. 128 (2022) 104417, https://doi.org/10.1016/j.cemconcomp.2022.104417.
[39] B.S. EN, 197-1, Cement-Part 1: Composition, Specifications and Conformity Criteria for Common Cements, European Committee For Standardisation, London, 2011.
[40] B.S. EN 196-3, Methods of Testing Cement - Determination of Setting times and Soundness, British Standards Institution (2016).
[41] B.S.. EN, BS 882: 1992: Specification for Aggregates from Natural Sources for Concrete, London: British Standards Institution (1992).
[42] N. Singh, J. Raza, F. Colangelo, I. Farina, Advances in lightweight artificial aggregates: typologies, compositions, applications, and prospects for the future, Sustainability 16 (2024).
[43] B.S.. EN, 13055-1: 2002; Lightweight Aggregates—Part 1: Lightweight Aggregates for Concrete, Mortar and Grout, British Standard Institution, London, UK (2002).
[44] B.S. EN, 934-2 "Admixtures For Concrete, Mortar and Grout-Part 2: Concrete Admixtures; Definitions, Requirements, Conformity, Marking and Labelling, British Standards Institution, 2009.
[45] ACI. 211.2-98, Standard Practice for Selecting Proportions for Structural Lightweight Concrete, ACI 211, American Concrete Institute, Farmington Hills, MI, USA, 2004, pp. 2–98.
[46] B.S. EN, 12350-2: 2009. Testing Fresh Concrete. Slump-test, British Standard Institution, London, UK, 2009.
[47] B.S. EN 206, Concrete-Specification, performance, production and conformity, BS EN 206:2013+A1:2021, British Standards Institution, 2021.
[48] B.S. EN, 1881-125. Testing Concrete. Methods for Mixing and Sampling Fresh Concrete in the Laboratory, British Standards Institution, London, UK, 2013.
[49] B.S. EN, 12390-2, "Testing hardened concrete-Part 2: Making and curing specimens for strength tests, British Standard Institute, London, 2009.
[50] B. EN, Testing Hardened Concrete—Compressive Strength of Test Specimens, BS EN 12390-3, British Standard Institution, London, UK, 2009.
[51] B. EN, Testing Hardened Concrete, 12390-6:, in: Tensile Splitting Strength of Test Specimens, 2009, British Standard Institution, London, 2009.

[52] B. EN, Testing Hardened Concrete—part 13: Determination of Secant Modulus of Elasticity in Compression. 12390-13, BSI—Br Stand Inst (2009).
[53] B. EN, Testing Hardened Concrete—Flexural strength of Test Specimens, BS EN 12390-5, British Standard: London, UK (2009).
[54] A. Saradar, P. Nemati, A.S. Paskiabi, M.M. Moein, H. Moez, E.H. Vishki, Prediction of mechanical properties of lightweight basalt fiber reinforced concrete silica fume and fly ash: experimental and numerical assessment, J. Build. Eng. 32 (2020) 101732.
[55] B. Zhang, Y. Feng, J. Xie, J. He, T. Yu, C. Cai, D. Huang, Compressive behaviours, splitting properties, and workability of lightweight cement concrete: the role of fibres, Constr. Build. Mater. 320 (2022) 126237.
[56] B.F..J.P. and S.R.. José Alexandre Bogas, Compressive Strength and Structural Efficiency of Structural Lightweight Aggregate Concrete: Throughout a compressive strength biphasic behaviour, in: The Third Intl. Conf. on Advances in Civil, Structural and Construction Engineering - CSCE 2015, Institute of Research Engineers and Doctors, USA, 2015.
[57] L. Domagała, A. Podolska, Effect of lightweight aggregate impregnation on selected concrete properties, Materials 15 (2021) 198.
[58] A.E. Richardson, Compressive strength of concrete with polypropylene fibre additions, Struct. Surv. 24 (2006) 138–153.
[59] A. Chajec, K. Krzywiński, Ł. Sadowski, K. Ostrowski, The influence of polypropylene fibres on the properties of fresh and hardened concrete, Tech. Trans. 2019 (2019) 71–82.
[60] Q. Fu, W. Xu, M. Bu, B. Guo, D. Niu, Effect and action mechanism of fibers on mechanical behavior of hybrid basalt-polypropylene fiber-reinforced concrete, Structures 34 (2021) 3596–3610, https://doi.org/10.1016/j.istruc.2021.09.097.
[61] S. Yan, Q. Dong, X. Chen, J. Li, X. Wang, B. Shi, An experimental and numerical study on the hybrid effect of basalt fiber and polypropylene fiber on the impact toughness of fiber reinforced concrete, Constr. Build. Mater. 411 (2024) 134270, https://doi.org/10.1016/j.conbuildmat.2023.134270.
[62] Y. Zhang, X. Sun, An investigation of the hybrid effect of pre-absorbed lightweight aggregate and basalt-polypropylene fiber on concrete performance, Constr. Build. Mater. 408 (2023) 133626.
[63] Y. Zeng, X. Zhou, A. Tang, P. Sun, Mechanical properties of chopped basalt fiber-reinforced lightweight aggregate concrete and chopped polyacrylonitrile fiber reinforced lightweight aggregate concrete, Materials 13 (2020) 1715.
[64] Ministry of Housing and Urban-Rural Construction of the People's Republic of China., Technical Specification for Lightweight Aggregate Concrete, China Building Industry Press: Beijing, China, 2002.
[65] D. Wang, Y. Ju, H. Shen, L. Xu, Mechanical properties of high performance concrete reinforced with basalt fiber and polypropylene fiber, Constr. Build. Mater. 197 (2019) 464–473.
[66] Y. Zhang, Z. Fan, X. Zhu, Effect of multi-minerals on the mechanical behavior and pore structure of fiber reinforced internal-cured green concrete, J. Clean. Prod. 359 (2022) 132075.
[67] C. Jiang, K. Fan, F. Wu, D. Chen, Experimental study on the mechanical properties and microstructure of chopped basalt fibre reinforced concrete, Mater. Des. 58 (2014) 187–193.
[68] J. Li, J. Niu, C. Wan, X. Liu, Z. Jin, Comparison of flexural property between high performance polypropylene fiber reinforced lightweight aggregate concrete and steel fiber reinforced lightweight aggregate concrete, Constr. Build. Mater. 157 (2017) 729–736.
[69] J.P. Romualdi, G.B. Batson, Mechanics of crack arrest in concrete, J. Eng. Mech. Div. 89 (1963) 147–168.
[70] ASTM C1609, Test Method for Flexural Performance of Fiber-Reinforced Concrete (Using Beam With Third-Point Loading), (2012). https://doi.org/10.1520/C1609_C1609M-12.
[71] ASTM C1018, Standard Test Method for Flexural Toughness and First-Crack Strength of Fiber-Reinforced Concrete (Using Beam With Third-Point Loading) 1997..
[72] K. Hannawi, H. Bian, W. Prince-Agbodjan, B. Raghavan, Effect of different types of fibers on the microstructure and the mechanical behavior of ultra-high performance fiber-reinforced concretes, Compos. Part B Eng. 86 (2016) 214–220.